Progress in Neurobiology xxx (xxxx) xxx

Contents lists available at ScienceDirect

Progress in Neurobiology

journal homepage: www.elsevier.com/locate/pneurobio

Original Research Article

Latent brain state dynamics and cognitive flexibility in older adults

Byeongwook Lee [a,*], Weidong Cai [a], Christina B. Young [b], Rui Yuan [a], Sephira Ryman [b], Jeehyun Kim [b], Veronica Santini [b], Victor W. Henderson [b,c], Kathleen L. Poston [b,d,e], Vinod Menon [a,b,e,*]

[a] Department of Psychiatry & Behavioral Sciences, Stanford University, Stanford, CA, 94305, United States
[b] Department of Neurology & Neurological Sciences, Stanford University, Stanford, CA, 94305, United States
[c] Department of Epidemiology & Population Health, Stanford University, Stanford, CA, 94305, United States
[d] Department of Neurosurgery, Stanford University, Stanford, CA, 94305, United States
[e] Stanford Neurosciences Institute, Stanford University, Stanford, CA, 94305, United States

ARTICLE INFO

Keywords:
Cognitive aging
Sternberg working memory task
Bayesian models
Latent brain state dynamics
Cognitive flexibility
Mediation

ABSTRACT

Cognitive impairment in older adults is a rapidly growing public health concern as the elderly population dramatically grows worldwide. While it is generally assumed that cognitive deficits in older adults are associated with reduced brain flexibility, quantitative evidence has been lacking. Here, we investigate brain flexibility in healthy older adults (ages 60–85) using a novel Bayesian switching dynamical system algorithm and ultrafast temporal resolution (TR = 490 ms) whole-brain fMRI data during performance of a Sternberg working memory task. We identify latent brain states and characterize their dynamic temporal properties, including state transitions, associated with encoding, maintenance, and retrieval. Crucially, we demonstrate that brain inflexibility is associated with slower and more fragmented transitions between latent brain states, and that brain inflexibility mediates the relation between age and cognitive inflexibility. Our study provides a novel neurocomputational framework for investigating latent dynamic circuit processes underlying brain flexibility and cognition in the context of aging.

1. Introduction

As the elderly population grows dramatically all over the world, there is an urgent need to understand the neural underpinnings of age-related cognitive deficits. Age-related cognitive changes in older adults occur even in the absence of brain disease with substantial variability in the extent and prevalence of age-related cognitive changes in older adults (Park et al., 2002; Hedden and Gabrieli, 2004; Salthouse, 2010, 2012; Samu et al., 2017). Furthermore, the incidence of Alzheimer's and other dementias increases rapidly in individuals over the age of 60 years (Rocca et al., 2011). Consequently, the need for investigations of mechanisms underlying individual differences in cognitive aging, the decline in cognitive processing that occurs as people get older, has taken on added significance (Salthouse, 2009; Hofer and Alwin, 2008]. Optimal cognitive functioning relies on dynamic and flexible reconfiguration of brain circuits (or latent brain states) that transiently link distributed brain regions in response to changing task demands (Braun et al., 2015; Finc et al., 2020; Bassett et al., 2011; Murphy et al., 2020; Cohen and D'Esposito, 2016; Taghia et al., 2018). However, little is known about how brain flexibility changes with age during a later life-span period in which cognitive deficits may occur before the onset of dementias. While it is generally assumed that cognitive deficits in older adults are related to reduced brain flexibility, direct quantitative evidence to support these claims has been lacking. Here, we identify novel measures of brain flexibility by characterizing dynamic temporal properties of latent brain states, including their context-specific occupancies and dynamic transitions, and determine how brain flexibility changes with age in a group of healthy older adults and in relation to cognition.

Investigations of brain inflexibility arising from time-varying and context-dependent brain states has been limited thus far because of challenges inherent to the complexities of nonlinear and latent dynamical processes that characterize brain function (Braun et al., 2015; Vidaurre et al., 2017; Kitzbichler et al., 2011; Cribben et al., 2012; Spadone et al., 2015; Shine et al., 2016; Lainscsek et al., 2019). To address these challenges, we used a novel Bayesian Switching Dynamic System (BSDS) (Taghia et al., 2018) with high-temporal resolution (TR

* Corresponding authors at: 401 Quarry Rd., Stanford University, Stanford, CA, 94305, United States.
E-mail addresses: bwlee89@stanford.edu (B. Lee), menon@stanford.edu (V. Menon).

https://doi.org/10.1016/j.pneurobio.2021.102180
Received 19 April 2021; Received in revised form 24 August 2021; Accepted 4 October 2021
Available online 7 October 2021

= 490 ms) fMRI data to determine hidden (latent) brain states and their dynamic transitions. Briefly, BSDS implements an unsupervised learning algorithm for determining latent brain states and dynamic state transitions from observed data (Taghia et al., 2018). Importantly, BSDS does not require arbitrary moving windows nor does it impose temporal boundaries associated with predefined task conditions, which are the major limitations of existing methods for probing context-dependent dynamic processes in the brain (Leonardi and Van De Ville, 2015; Shakil et al., 2016). Each latent brain state is associated with a unique dynamic process that captures time-varying activation and functional connectivity in an optimal latent subspace. Crucially, this approach can capture dynamic temporal properties of brain states, their occurrence rates and relation to different phases of working memory, probability of state transitions, and dynamic changes in the underlying functional circuitry.

Diminished ability to adaptively maintain and manipulate information is a main component of cognitive aging (Braver and West, 2008). Deficits in working memory are associated with inability to flexibly engage cognitive control systems in order to inhibit irrelevant stimuli and switch between tasks (Braver and West, 2008; Reuter-Lorenz and Sylvester, 2005; Gazzaley et al., 2005; Borella et al., 2008). Ultimately, deficits in working memory impact cognitive flexibility (Dajani and Uddin, 2015), a higher-order meta-control ability to adapt behavior in response to changes in the environment (Scott, 1962). Both working memory and cognitive flexibility involve a widely distributed cortical-subcortical system, including dorsolateral prefrontal cortex (DLPFC), dorsomedial prefrontal cortex (DMPFC), anterior insula (AI), posterior parietal cortex (PPC), caudate (Cau) and thalamus (Cai et al., 2014; Kim et al., 2012; Cai et al., 2019; Rottschy et al., 2012; Owen et al., 2005), and age-related functional alterations have been observed in this same cortical-subcortical system (Keller et al., 2015). However, little is known about how cognitive flexibility is related to latent brain state dynamics underlying working memory in healthy older adults.

Here we investigate latent brain state dynamics of a cortical-subcortical cognitive control network associated with performance of a Sternberg working memory task in the context of aging. Participants were presented with a set of visual stimuli during an encoding phase and asked to remember the stimuli after a brief delay period. Because the Sternberg working memory task consists of distinct task phases, it is an ideal paradigm for investigating the dynamical evolution of brain states and their modulation with cognitive demand. BSDS analysis of ultra-fast fMRI allowed us to identify latent brain states and several key dynamic temporal properties associated with Sternberg working memory task performance: (i) posterior probability of each latent state, which provides probabilistic information regarding the likelihood of a certain latent brain state occurring at a given time, (ii) occupancy rate and mean lifetime, which quantify the occurrence of each latent brain state in each condition and phase of the working memory task, (iii) state transition matrix and switch paths, which provide information regarding how latent brain states transition from one state to another, and (iv) functional brain circuits associated with each latent brain state. In sum, our approach using the event-related fMRI design with high temporal resolution allowed us to more directly investigate, in a quantitively rigorous manner, age-related changes in cognitive and brain flexibility associated with working memory, and overcome limitations of resting-state fMRI studies (Escrichs et al., 2021; Ezaki et al., 2018) which

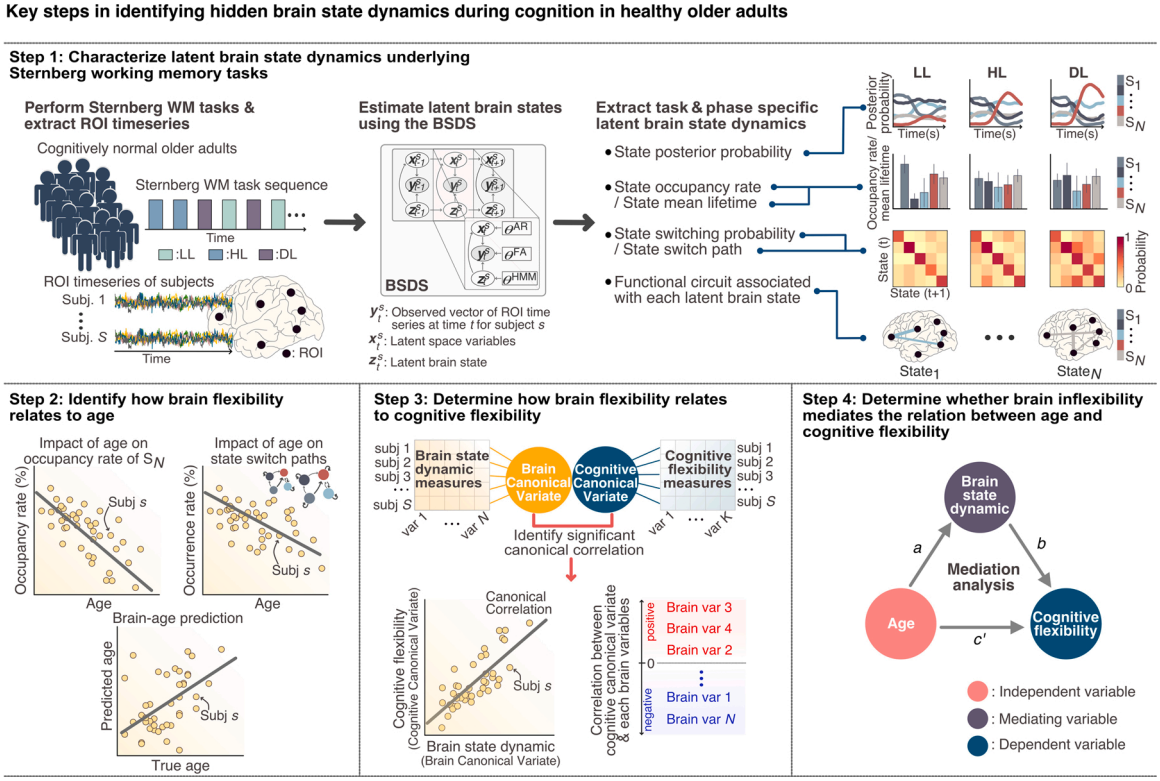

Fig. 1. Overall analysis approach for identifying latent brain state dynamics and its relation to age and cognitive flexibility. Our approach is composed of four analysis steps. In Step 1, we used the Bayesian switching dynamical system (BSDS) model to determine the evolution of dynamic latent brain states underlying the Sternberg working memory (WM) task. We identified latent brain states (S_1 … S_N) and characterized their dynamic properties, including (1) posterior probability, (2) occupancy rate and mean lifetime, (3) state switching probability and state switch paths, and (4) functional circuit associated with each latent brain state. In Step 2, we examined how brain flexibility, quantified based on dynamic properties of latent brain states, changes with age in a group of healthy older adults. In Step 3, we determined how brain flexibility relates to cognitive flexibility using canonical correlation analysis with cross-validation and prediction analysis based on brain state properties obtained in Step 1 and neuropsychological measures of cognitive flexibility. In Step 4, we determined whether brain inflexibility mediates the relation between age and cognitive flexibility in healthy older adults.

cannot directly assess cognitive functioning.

Our study addresses five main goals (Fig. 1). Our first goal was to identify latent brain states and characterize dynamic state changes associated with cognitive load and distinct phases of the Sternberg working memory task in healthy older adults using BSDS. We hypothesized that there are multiple latent brain states underlying working memory and that examination of latent brain state properties would reveal dynamic state changes that map onto and are constrained by task context (Taghia et al., 2018). We further hypothesized that latent brain states critical for working memory would be associated with increased cortical-subcortical interactions (Chang et al., 2007; McNab and Klingberg, 2008). The second goal of our study was to identify functional circuits associated with latent brain states as a function of cognitive load and distinct phases of the Sternberg working memory task. Third, we derived quantitative measures from latent brain state dynamics that characterize brain flexibility and then used a dimensional approach to determine how brain flexibility is impacted by age in healthy older adults. We hypothesized that dynamical load-dependent measures of latent brain states would characterize brain flexibility in healthy older adults and that flexible engagement of latent brain states would be negatively impacted by age. The fourth goal of our study was to investigate how brain inflexibility impacts cognitive inflexibility. We hypothesized that latent brain state properties associated with brain inflexibility would predict cognitive flexibility assessed with standardized neuropsychological assessments. Our final goal was to determine how changes in brain inflexibility with age impact cognitive flexibility. We hypothesized that reduced brain flexibility with age would emerge as a mediator of reduced cognitive flexibility in older adults. Our novel neurocomputational framework provides new insights into latent dynamic circuit processes underlying brain and cognitive flexibility in the context of aging.

2. Materials and methods

2.1. Participants

Participants were enrolled in the Stanford Alzheimer's Disease Research Center. During clinical consensus meeting, all participants were adjudicated as neurologically and cognitively normal after completing formal neurological examination, comprehensive neuropsychological battery and clinical history by a licensed neurologist. Additional inclusion criteria were $>$ 60 years of age and neuropsychological testing within 6 months of the fMRI session. A total of 44 cognitively normal older adults (age: 71.57 $\pm$ 5.68 years, range 60–85 years; 26 females, 18 males; Table S1) with maximum head displacement less than 3 mm (average framewise displacement $<$0.2 mm) were included in the final analyses. Average framewise displacement was not correlated with age ($r = 0.24$, $p = 0.12$, *Pearson*'s correlation). All participants provided written consent and the Stanford University Institutional Review Board approved all study protocols.

2.2. Experimental procedures

Participants performed a modified Sternberg working memory task (Poston et al., 2016) during fMRI. Each trial consisted of either low-load (LL), high-load (HL), or distractor-load (DL) working memory conditions. Each trial began with fixation (0.5 s) followed by an encoding phase (2 s) during which a set of stimuli was simultaneously displayed. The set of stimuli consisted of 5 identical numbers (LL condition), 5 different numbers (HL condition), and 5 different numbers along with 5 different characters (DL condition). The trial was then followed by a maintenance phase (6 $\pm$ 2 s), during which a fixed marker was displayed, and the presentation of a probe for 0.5 s. Participants indicated whether the probe matched any of the numbers displayed during the encoding phase. Accuracy and reaction time (RT) were recorded for each trial. Each scan included 4 task runs, where each consisted of 6 LL, 6 HL, and 6 DL working memory trials randomly intermixed. The stimulus presentations were implemented using E-Prime software (v2.0; Psychology Software Tools, Pittsburgh, PA; 2002) and projected at the center of the screen using a magnet-compatible projection system. Prior to each fMRI session, participants were trained with instructions and completed a practice session of the task.

2.3. Neuropsychological tests

To assess cognitive flexibility, participants completed the Trail Making Test (TMT) and Victoria Stroop Test, which are widely used neuropsychological instruments. The TMT consisted of two parts. In part A, participants rapidly connect a set of 25 dots in order (1-2-3…) while maintaining accuracy, whereas in part B, participants rapidly alternate between numbers and letters (1-A-2-B…). Part A measures processing speed while Part B measures processing speed and attention switching. We also computed the *B-A* time difference time, which provides a relatively pure indicator of executive control ability (Sánchez-Cubillo et al., 2009). The Victoria Stroop Test consisted of three parts. In the first part (Dot test), a grid of colored dots was presented and participants rapidly named the color; In the second part (Word test), a grid of words printed in black ink was presented and participants rapidly read the words; In the third part (Colored-word test), a grid of color names printed in colors not corresponding to the words (e.g., the word "red" printed in green ink) was presented and participants were asked to rapidly name the color of the words. The first (Dot test) and second (Word test) parts measure processing speed, while the third part (Colored-word test) measures selective inhibition. The scores of TMT and Stroop Test represent task completion times, such that low score indicates good performance and high score indicates poor performance.

Participants also completed three additional neuropsychological tests that assessed other aspects of cognition unrelated to cognitive flexibility. First, a story memory test (Craft et al., 1996) was used to assess episodic memory. Second, a complex figure copy (Possin et al., 2011) was used to assess visuospatial ability. Third, a confrontation naming test (Ivanova et al., 2013) was used to assess language ability.

2.4. fMRI acquisition and preprocessing

The fMRI images were collected using a 3 T scanner. A total of 790 functional images were acquired using multiband echo-planar imaging with the following parameters: 47 slices, repetition time (TR) = 490 ms, flip angle 45 °, echo time = 30 ms, field of view = 220 × 220 mm, matrix = 74 × 74, 3 mm slice thickness, and voxel size = 2.97 × 2.97 × 3 mm. The first 12 time points were removed to allow for signal equilibration, leaving 778 time points for each subject. Each subject's T1-weighted anatomical scan had been acquired using a magnetization-prepared rapid-acquisition gradient echo (MPRAGE) sequence (256 slices with a 176*256 matrix; voxel size 1.00 × 0.977 × 0.977mm^3). All functional MRI data were preprocessed using SPM12 (http://www.fil.ion.ucl.ac.uk/spm/software/spm12/), as well as in-house programs in MATLAB (MathWorks). Functional MRI data were first slice time corrected, aligned to the averaged time frame to correct for head motion, and co-registered with each participant's T1-weighted images. Structural MRI images were segmented into grey matter, white matter, and cerebrospinal fluid. Using the transformation matrix derived from the T1-weighted anatomical brain images, the functional images were then transformed to the standard Montreal Neurological Institute (MNI) template in 2 × 2 × 2 mm^3 with the Diffeomorphic Anatomical Registration Through Exponentiated Lie algebra (DARTEL, Ashburner et al. 2007) toolbox. A 6-mm Gaussian kernel was used to spatially smooth the functional images. Subjects with more than 3 mm head motions were excluded.

2.5. Time series from regions of interest

To define the regions of interest (ROIs), we first examined whole-brain activation patterns associated with the Sternberg DL vs. LL and HL vs. LL contrasts. Consistent with previous studies (Chang et al., 2007; Altamura et al., 2007; Heinzel et al., 2016), the Sternberg task strongly activated prefrontal and parietal regions implicated in cognitive control and working memory (Menon and D'Esposito, 2021), as well as the thalamus and caudate. The Brainnetome atlas (Fan et al., 2016) was used to demarcate ROIs in: (1) left posterior parietal cortex (lPPC), (2) right posterior parietal cortex (rPPC), (3) left dorsolateral prefrontal cortex (lDLPFC), (4) right dorsolateral prefrontal cortex (rDLPFC), (5) bilateral dorsomedial prefrontal cortex (DMPFC), (6) left anterior insula (lAI), (7) right anterior insula (rAI), (8) left caudate (lCau), (9) right caudate (rCau), (10) left thalamus (lThalamus), (11) right thalamus (rThalamus). The time series of each ROI was calculated by taking the average of the time series of all voxels within each ROI. A multiple linear regression approach with 6 realignment parameters (3 translations and 3 rotations) was applied to account for head motion-related artifacts and the resulting time series were further linearly detrended, normalized, and high-pass filtered (>0.008 Hz).

To examine the robustness of our findings with respect to ROI selection, we conducted additional analyses using cognitive control and working memory-related brain regions. Task-relevant brain regions involved in cognitive control were defined using functional clusters from an independent study in which brain networks were derived using independent component analysis on resting-state fMRI (Shirer et al., 2012). Networks of interest included the salience network, fronto-parietal network, default mode network and dorsal attention network, from which we chose the following ROIS: bilateral AI, bilateral DLPFC, bilateral FEF, bilateral PPC, PCC, VMPFC and right DMPFC (Fig. S6A).

2.6. Bayesian switching dynamical system model

BSDS is an unsupervised Bayesian learning algorithm that determines latent brain states and dynamic state transitions from observed data (Taghia et al., 2018). In general, BSDS examines time-series data to identify latent brain states that vary in their activation patterns over time as well as their inter-regional functional connectivity. More specifically, we applied a vector autoregressive (AR) (Fox, 2009) and factor analysis (FA) (Everett, 2013; Ghahramani and Hinton, 1996) models that can simultaneously estimate latent brain states in an optimal low dimensional subspace. Importantly, BSDS applies a hidden Markov model to latent space variables of the observed time-series data, resulting in a parsimonious model of generators underlying the observed data. Each estimated latent brain state is associated with a unique dynamic process that captures time-varying activation and inter-regional functional connectivity in an optimal latent subspace. BSDS does not require arbitrary moving windows, nor does it impose temporal boundaries associated with predefined task conditions, which are major limitations of existing methods for probing dynamic processes in the brain (Leonardi and Van De Ville, 2015; Shakil et al., 2016).

Here we briefly describe the mathematical framework of the BSDS model (Taghia et al., 2018). Let $\boldsymbol{y}_t^s$ denote a D-dimensional vector of ROI timeseries obtained from subject s in time t, where D is the number of ROIs. Following the general formulation of the switching state-space models, we defined z_t^s as the latent state variables and $\boldsymbol{x}_{kt}^s$ as the latent space variables associated to $\boldsymbol{y}_t^s$ at the k -th latent state, that is $z_{kt}^s = 1$. The z_t^s is a 1-of- K discrete vector with elements $z_{kt}^s, \forall k = 1, \ldots, K$. Two successive time instances are dependent through a 1st-order Markov chain of Hidden Markov Model (HMM). Using Markovian properties and given state transition probabilities $\boldsymbol{A}$, where $A_{jk} \equiv p(z_{tk}^s = 1 | z_{t-1,j}^s = 1)$ and a marginal distribution $p(z_1^s|\boldsymbol{\pi}) = \prod_{k=1}^{K} \pi_k^{z_{1k}^s}$ represented by a vector of initial probabilities $\boldsymbol{\pi}$ where $\pi_k \equiv p(z_{1k}^s = 1)$, the probability distribution for the latent state variables is expressed by $p(z_t^s|z_{t-1}^s, \boldsymbol{A}) = \prod_{k=1}^{K}\prod_{j=1}^{K} A_{jk}^{z_{t-1,j}^s z_{tk}^s}$ for all $t > 1$. We assume that at a given latent state k in time t, shown by $z_{kt}^s = 1$, the observed vector $\boldsymbol{y}_t^s$ is generated via probabilistic interpretation of a factor analysis model (Everett, 2013; Ghahramani and Hinton, 1996) as:

$$\boldsymbol{y}_t^s = \boldsymbol{U}_k \boldsymbol{x}_{kt}^s + \boldsymbol{\mu}_k + \boldsymbol{e}_{kt}, \ \forall t \ | z_{kt}^s = 1$$

where $\boldsymbol{U}_k$ is a $D \times P$ dimensional linear transformation matrix, where the P is the dimensionality of the latent space variable (in general $P < D$), $\boldsymbol{\mu}_k$ is the overall bias, and $\boldsymbol{e}_{kt}$ is the measurement noise. With the normality assumption, that is $\boldsymbol{x}_{kt}^s \sim \mathcal{N}(0, 1)$ and $\boldsymbol{e}_{kt} \sim \mathcal{N}(0, \boldsymbol{\Psi}_k)$, the marginal distribution of $\boldsymbol{y}_t^s$ follows a Gaussian distribution as $p(\boldsymbol{y}_t^s|\boldsymbol{\mu}_k, \boldsymbol{U}_k, \boldsymbol{\Psi}_k) = \mathcal{N}(\boldsymbol{\mu}_k, \boldsymbol{U}_k \boldsymbol{U}_k{}^T + \boldsymbol{\Psi}_k)$ where T denotes the transpose operator. We then define a dynamical process on the latent space variables using an autoregressive (AR) model (Fox, 2009) of order R as:

$$\boldsymbol{x}_{kt}^s = \overline{\boldsymbol{X}}_{kt}^s \overrightarrow{V_k} + \boldsymbol{\varepsilon}_{kt}, \ \forall t \ | z_{kt}^s = 1$$

where $\overrightarrow{V_k}$ is a vector of AR coefficients. $\overline{\boldsymbol{X}}_{kt}^s = \mathrm{diag}(\overline{\boldsymbol{x}}_{kt}^s)$ is a block diagonal isotropic matrix with elements of $\overline{\boldsymbol{x}}_{kt}^s = \left(\overline{\boldsymbol{x}}_{k,t-1}^s{}^{\mathrm{T}}, \overline{\boldsymbol{x}}_{k,t-2}^s{}^{\mathrm{T}}, \ldots, \overline{\boldsymbol{x}}_{k,t-R}^s{}^{\mathrm{T}}\right)$ represented using latent space variables from the previous R time frames. $\boldsymbol{\varepsilon}_{kt} \sim \mathcal{N}(\mathbf{m}_k, \Sigma_k)$ is the remaining error term in the latent space. All analyses conducted in this study use a 1st-order AR model ($R = 1$). BSDS was initialized with 10 states and it converged to 5 states. Detailed theoretical derivations are provided in the previous study (Taghia et al., 2018).

2.7. Temporal properties of latent brain states

BSDS estimated the posterior probability of each latent brain state at each time point and chose the latent brain state with highest probability as the dominant state at that time point. Using the temporal evolution of the latent brain states, we measured temporal properties of each latent brain state in each task condition (LL, HL, and DL), including occupancy rate, mean lifetime, and state switching probability. Occupancy rate quantifies the proportion of time that a state is chosen as the dominant state. Mean lifetime quantifies the average duration that the state persists as a dominant state before switching to another state. State switching probability quantifies the chance that brain state at time point t either remains at its own state or switches to another brain state at the time point $t + 1$. These temporal properties were examined to characterize each task condition and further used to examine their relationship with age and behavioral performances. Further details are provided in Supplementary Methods.

2.8. Task and phase prediction using time-varying latent brain state dynamics

Task classification analysis was performed to investigate whether time-varying latent brain state dynamics contain task-specific information. We built a multiclass classifier based on a linear support vector machine using the MATLAB package LIBSVM (http://www.csie.ntu.edu.tw/~cjlin/libsvm) (Chang and Lin, 2001) to discriminate task conditions at each time point. The averaged posterior probabilities of the latent brain states at each time point were used as features to train the classifier. Classifier performance was evaluated by conducting leave-one-out cross-validation (LOOCV) analysis. Specifically, posterior probability time series of the five latent brain states from one participant were used as a test set and the posterior probability time series of the

brain states obtained from the rest of the participants were used to train the classifier. Then, the trained classifier was applied to the test set to predict moment-by-moment correspondence between posterior probabilities of the latent brain states and task conditions (LL, HL, and DL). This procedure was performed *S* times (*S*: number of participants), and the cross-validation accuracy across the test set was used to evaluate the performance of the classifier. We further evaluated statistical significance of LOOCV accuracy using permutation test (5,000 times). We also examined whether time-varying latent brain state dynamics contain phase-specific information by performing phase classification analysis in each load condition using the same analytic procedure as described above.

2.9. Dynamic functional connections that distinguish latent brain states

To identify dynamic functional connections that distinguish each latent brain state, a feature identification analysis was performed on the covariance matrix estimated from the BSDS analysis. We first performed logistic regression on feature matrix with Elastic-net regularized generalized linear model using the MATALB package Glmnet (https://web.stanford.edu/~hastie/glmnet_matlab/) (Qian et al., 2013) to distinguish brain states. A lambda optimization was done by conducting a 10-fold cross-validation to minimize misclassification error. Then, the optimized lambda was applied on the full data set and connections with nonzero weights were selected. Next, we performed a univariate analysis on the chosen connections and examined connections that are significantly different between latent brain states. Lastly, we examined whether the connection pattern of each latent brain state is enough to distinguish brain states. It was done by training logistic regression classifier and evaluating the performance using LOOCV. Statistical significance of LOOCV accuracy was further evaluated using permutation test (5,000 times).

2.10. Latent brain state dynamics in relation to cognitive flexibility

To examine whether the latent brain state dynamics underlying working memory are associated with cognitive flexibility, we conducted canonical correlation analysis (CCA). CCA is a powerful statistical method for examining the relationship between two multivariate sets of variables by finding an optimal linear combination for each of the sets (referred to as canonical variates) that maximizes the relation between the two multivariate sets. The set of brain variables consisted of mean lifetimes of the latent brain states under three task load conditions (LL, HL, and DL). The set of cognitive variables consisted of TMT_A Time, TMT_{B-A} Time and Stroop Color-Word Time, which reflects processing speed, attention switching, and selective inhibition, respectively. Next, prediction analysis was performed using LOOCV. Pearson's correlation was used to evaluate the correlation between the predicted brain and cognitive variables. The statistical significance of the correlation was evaluated using permutation tests (1,000 times). All analyses controlled for sex and education level. Further details are provided in Supplementary Methods.

2.11. Mediation effect of brain state dynamics on the relation between age and cognitive flexibility

To investigate whether the cognitive deficits in older adults are mediated by brain state dynamics, we conducted mediation analysis. Mediation analysis examines whether a covariance between two variables (*X* and *Y*) can be explained by a mediating (*M*) variable. In this study, we examined the relationship between age (*X*), cognitive flexibility (*Y*), and brain state dynamics (*M*) while controlling for sex and education level from the variables *Y* and *M*. Specifically, we examined the total effect of *X* on *Y* (path *c*), the relationship between *X* and *M* (path *a*), the relationship between *M* and *Y* (path *b*), and the direct effect of *X* on *Y* after including *M* as a mediator in the model (path *c'*). The significance of the indirect effect of *X* on *Y* through the *M* (i.e., path *axb*) was tested using a bootstrapping procedure. This approach included calculating unstandardized indirect effects for each of 10,000 bootstrapped samples and then calculating the 95 % confidence interval. The significance of the indirect effect was evaluated using bootstrapped confidence intervals within the R package *"mediation"* (https://cran.r-project.org/web/packages/mediation/).

3. Results

3.1. Behavior: working memory performance, cognitive flexibility, and age

Forty-four cognitively healthy older adults (71.36 years old, 26 females/18 males) performed a modified Sternberg working memory task during fMRI (Poston et al., 2016). The Sternberg task included three load conditions, low-load (LL), high-load (HL), and distractor-load (DL), that required low, medium, and high levels of cognitive demand, respectively. For each trial, participants viewed a set of stimuli for 2 s (encoding phase), a jittered delay varying between 4 and 8 s (maintenance phase), and a probe prompting participants to determine whether the probe was one of the stimuli (retrieval phase) (Fig. 2A). This paradigm allowed us to investigate the effects of cognitive load (LL, HL, and DL) and working memory phases (encoding, maintenance and retrieval) on intra-trial dynamics. Each participant completed four runs of the Sternberg task, with each run consisting of 6 trials per task condition in random order. Accuracy and reaction time (RT) were recorded for each trial.

Average accuracy in the LL condition (96.8 ± 4.1 %) was significantly higher than HL (91.7 ± 5.4 %) [$t_{(43)} = 5.64$, $p < 0.001$, *Cohen's* $d = 1.07$, paired *t*-test] and DL (93.1 ± 9.3 %) [$t_{(43)} = 2.51$, $p < 0.05$, *Cohen's* $d = 0.55$, paired *t*-test] conditions (Fig. 2B). Average RT in the LL condition (1.00 ± 0.22 s) was also significantly faster than HL (1.28 ± 0.24 s) [$t_{(43)}$=-13.27, $p < 0.001$, *Cohen's* $d = 1.22$, paired *t*-test] and DL (1.29 ± 0.25 s) [$t_{(43)}$=-13.74, $p < 0.001$, *Cohen's* $d = 1.23$, paired *t*-test] conditions (Fig. 2B, Table S1). No significant differences in accuracy or RT were found between HL and DL conditions (all *ps*>0.3). Thus, participants performed well on the Sternberg task and demonstrated a load effect. Age was marginally correlated with accuracy in the DL condition (r=-0.28, $p = 0.07$, *Pearson*'s correlation) but not LL and HL conditions (*ps*>0.05). Age was not correlated with RT in any condition (all *ps*>0.3) (Fig. 2B, Table S1)

Participants also completed the Trail Making Test (TMT) (Bowie and Harvey, 2006) and Victoria Stroop Test (Stroop, 1935) outside the scanner. The TMT and Stroop Test assessed processing speed, attention switching, and inhibition, and were not correlated with age (all *ps*>0.3, Table S1). TMT and Stroop tasks provide comprehensive measures for different components of cognitive flexibility (Dajani and Uddin, 2015; Scott, 1962). Taken together, performance on the Sternberg working memory task, TMT and Stroop task were not directly related to age in this group of healthy older adults, but were rather indirectly related as demonstrated below.

3.2. Latent brain states during working memory

Functional MRI data was acquired using a multiband EPI protocol with high temporal resolution (TR = 490 ms), which enhances the power to model brain circuit dynamics. We applied BSDS to time series extracted from 11 brain regions of interest (ROIs), which are determined by activation associated with a strong load effect (Fig. 2C). Consistent with previous studies of working memory (Taghia et al., 2018; Chang et al., 2007; D'Esposito and Postle, 2015; Goldman-Rakic, 1995; Myers et al., 2017), the ROIs include bilateral posterior parietal cortex (PPC), dorsolateral prefrontal cortex (DLPFC), dorsomedial prefrontal cortex (DMPFC), anterior insula (AI), caudate (Cau), and thalamus. BSDS was used to determine key temporal properties of latent brain states

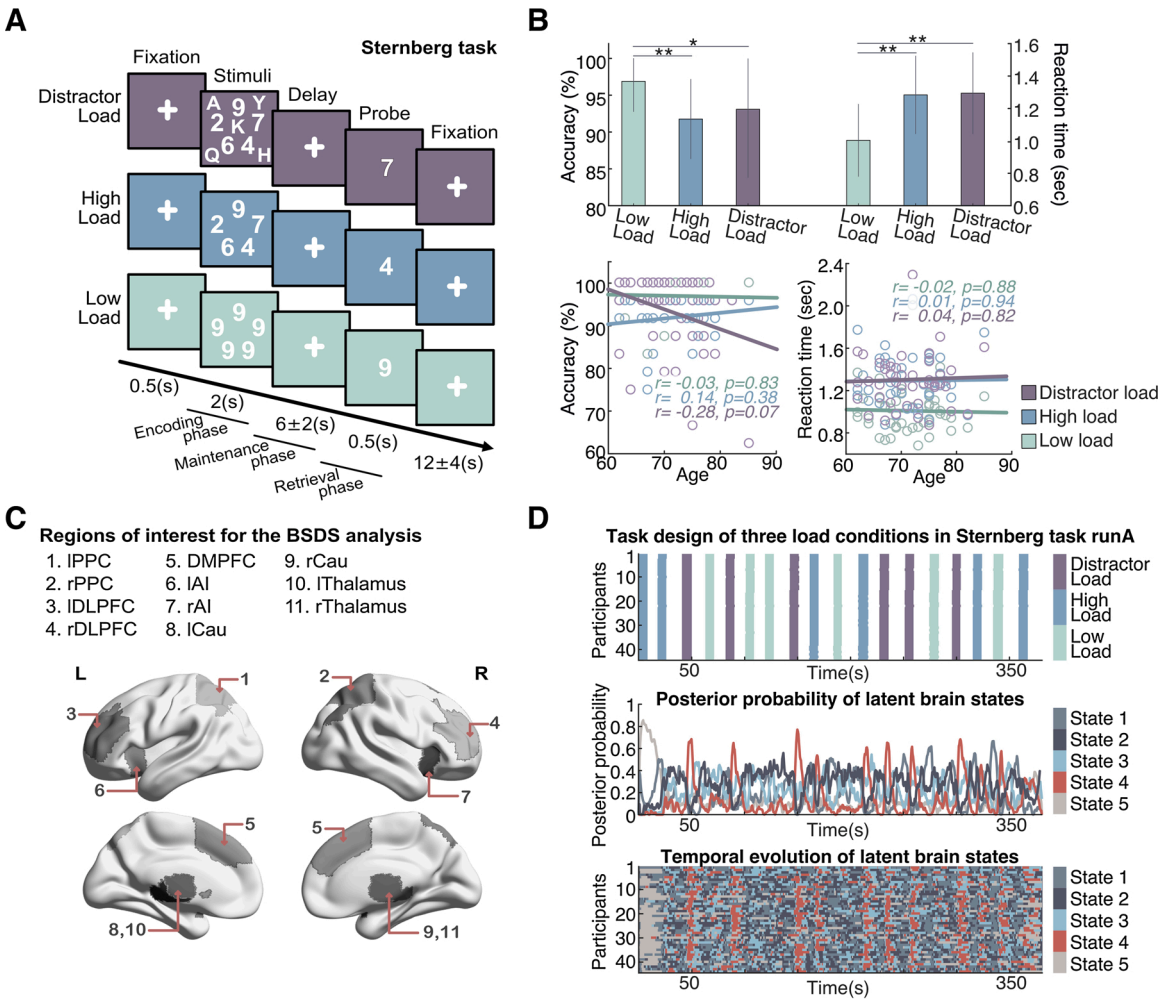

Fig. 2. Bayesian switching dynamical system (BSDS) analysis of Sternberg working memory task data. **(A)** Sternberg working memory paradigm with low-load (LL; 5 identical numbers), high-load (HL; 5 different numbers), and distractor-load (DL; 5 different numbers and 5 different letters) conditions. Each trial consisted of fixation (0.5 s), an encoding phase (2 s) with stimuli presentation, a maintenance phase (6 ± 2 s) during which a fixation cross is displayed, the presentation of a probe (0.5 s), and an intertrial interval (12 ± 4 s). During the probe, participants indicated whether the probe matched any number displayed during the encoding phase. **(B)** Accuracy and reaction time (RT) for the Sternberg working memory task. Accuracy and RT were significantly greater and faster, respectively, in the LL compared to HL and DL conditions (top). Accuracy and RT of all three load conditions were not associated with age (bottom). Data represent mean and standard deviation (mean ± SD). $*p < 0.05$, $**p < 0.001$. **(C)** Brain regions of interest used in BSDS analysis. **(D)** The scan session included 4 task runs, each consisting of 6 L L, 6 H L, and 6 DL randomly intermixed trials. Task design of the three load conditions in run A (top). Averaged time-varying posterior probability of the five latent brain states across the 44 participants (middle). Temporal evolution of the five latent brain states identified in each of the 44 participants (bottom).

including: (i) their time-varying posterior probabilities, (ii) occupancy rates and mean lifetime, (iii) transition probabilities and switch paths related to LL, HL and DL conditions, and (iv) difference in dynamic functional connectivity pattern between states.

3.3. Temporal properties of latent brain states: posterior probability distinguishes task conditions

BSDS revealed five latent brain states defined by their unique spatiotemporal properties. To facilitate interpretation of each brain state, the temporal properties of each latent brain state were examined. For each participant, BSDS estimated the posterior probability of each latent brain state at each time point (Fig. 2 D middle and Fig. S1), and the latent brain state with the highest posterior probability was chosen as the dominant state at that point for that participant (Fig. 2D bottom and Fig. S1). Across participants, each latent brain state showed distinct moment-by-moment changes in posterior probability across working memory trials and inter-trial-intervals (ITI) in the LL, HL, and DL task conditions (Fig. 3A–C).

To determine whether latent brain state dynamics (Fig. 3D) differentiates cognitive load conditions (i.e., LL, HL, DL), we conducted multivariate classification analyses using a Linear Support Vector Machine (LSVM) algorithm and leave-one-out cross-validation (LOOCV) (Chang and Lin, 2001). The classification models trained on posterior probabilities of latent brain states in each task accurately predicted load conditions on unseen data with greater than 50 % accuracy, which significantly exceeds the chance level of 33 % ($p < 0.001$, permutation test) (Fig. 3E). Interestingly, the posterior probability of latent brain states during the retrieval phase had the highest prediction accuracy in comparison to encoding and maintenance phases (72.2 %, $p = 0.002$, permutation test) (Fig. 3E), suggesting that the temporal properties of latent brain states are more differentiated during retrieval than encoding or maintenance (all $ps<0.001$, two-tailed t-test). These results demonstrate that the posterior probabilities of latent brain states can distinguish cognitive load.

3.4. Temporal properties of latent brain states: posterior probability distinguishes task phases

We next conducted multivariate classification analyses using the

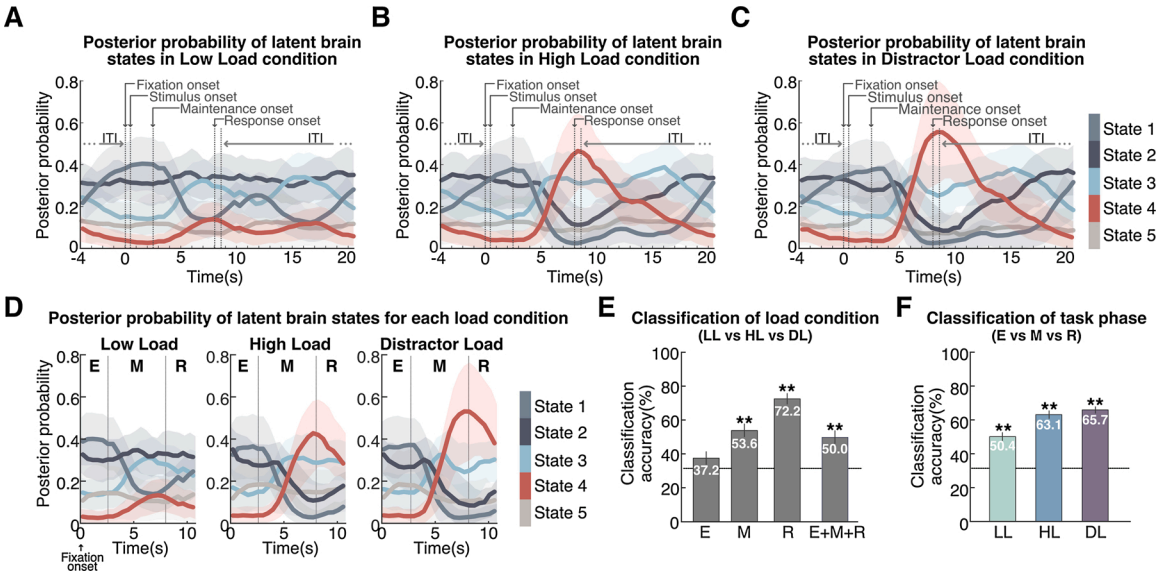

Fig. 3. Temporal evolution of latent brain states during Sternberg working memory task. Time-varying posterior probabilities of five latent brain states identified using BSDS associated with the **(A)** low-load (LL), **(B)** high-load (HL), and **(C)** distractor-load (DL) conditions. Temporal dynamics of each state are shown in relation to working memory trials and inter-trial-intervals (ITI). Each latent brain state showed distinct moment-by-moment changes in posterior probability before, during, and after engaging in the conditions. **(D)** Time-varying posterior probabilities of latent brain state corresponding to *Fixation Onset* to 1 s after *Response Onset*. Each task phase was separated by vertical dashed lines (E: Encoding, M: Maintenance, R: Retrieval). Posterior probability of each latent brain state showed distinct temporal profiles across different task phases. Notably, posterior probability of State 4 increased with cognitive load during maintenance and retrieval phases. **(E)** Classification analysis based on a linear SVM classifier. Time-varying posterior probability of latent brain states distinguished between LL, HL and DL conditions. Classification rate was highest in the retrieval phase (R), followed by maintenance (M) and encoding (E) phases. **(F)** Time-varying posterior probability of latent brain states distinguished between Encoding, Maintenance, and Retrieval phases of the working memory task. HL and DL conditions showed better classification accuracy compared to the LL condition. In **(E)** and **(F)**, the black horizontal line indicates the chance level (33.3 %). $^{**}p < 0.001$.

same LSVM algorithm and LOOCV to examine whether the posterior probability of latent brain states distinguishes between the encoding, maintenance, and retrieval phases of the task. Task phase classification accuracies were 50.4 %, 63.1 %, and 65.7 % in LL, HL and DL, respectively, and significantly above the chance level of 33 % (all $ps<0.001$, permutation test) (Fig. 3F), suggesting that temporal properties of latent brain states are more differentiated in HL and DL than LL conditions (all $ps<0.001$, two-tailed *t*-test). These results demonstrate that the posterior probabilities of latent brain states can distinguish working memory phase. Taken together with findings from the previous section, these results demonstrate that the posterior probabilities of latent brain states contain rich information that differentiates working memory phase and load.

3.5. Temporal properties of latent brain states: occupancy rate and mean lifetime across task conditions

We next examined occupancy rates and mean lifetimes for each load condition and each latent brain state. Occupancy rate quantifies the fraction of time a given state is most likely to occur, and mean lifetime quantifies the average dwelling time that a state persists before switching to another state. Examination of load effects on occupancy rate and mean lifetime revealed that these temporal properties were significantly higher in DL than HL and in HL than LL conditions for State 4 (all $ps<0.05$, two-tailed *t*-test, FDR-corrected), suggesting that State 4 is a key state associated with cognitive load (Fig. 4A and B). In contrast, occupancy rates and mean lifetimes of States 1 and 2 were significantly higher in the LL compared to both the HL and DL conditions (all $ps<0.05$, two-tailed *t*-test, FDR-corrected), but there was no difference between HL and DL conditions ($p > 0.05$, Fig. 4A and B). There was no significant difference between load conditions in State 3 ($ps > 0.05$, Fig. 4A and B). These results demonstrate that the latent brain states are characterized by unique load-dependent temporal properties.

3.6. Temporal properties of latent brain states: occupancy rate and mean lifetime across task phases

We then examined occupancy rate and mean lifetime of each latent brain state for each working memory task phase. During the encoding phase, States 1 and 2 had significantly higher occupancy rate and mean lifetime than other states in LL, HL, and DL conditions (all $ps<0.05$, two-tailed *t*-test, FDR-corrected) (Fig. 4C and F). During the maintenance and retrieval phases, States 3 and 4 had significantly higher occupancy rates and mean lifetimes than other states in HL and DL conditions (all $ps<0.05$, two-tailed *t*-test, FDR-corrected) (Fig. 4D, E, G and H). During ITI phase, States 2 and 3 had the highest occupancy rates and mean lifetimes (Fig. S2) (all $ps<0.05$, two-tailed *t*-test, FDR-corrected). Comparisons for each state across task phases revealed that the occupancy rate and mean lifetime of State 1 during the encoding phase was significantly higher than the maintenance and retrieval phases in all the load conditions (all $ps<0.05$, two-tailed *t*-test, FDR-corrected), suggesting that State 1 is more associated with information encoding. In contrast, the occupancy rates and mean lifetimes of State 3 and 4 were significantly higher during the maintenance and retrieval phases in comparison to the encoding phase (all $ps<0.05$, two-tailed *t*-test, FDR-corrected) (Fig. 4D, E, G and H). State 4 showed significant load-dependent increments in occupancy rate and mean lifetime from LL to HL and from HL to DL in both maintenance and retrieval phases (all $ps<0.05$, two-tailed *t*-test, FDR-corrected), whereas State 3 did not show significant load-dependent changes in its occupancy rate and mean lifetime. This suggests that State 4 is modulated by cognitive load for maintaining and retrieving information. Finally, the occupancy rate of State 5 remained low (under 15 %) across all the task phases and conditions, but was more likely to occur at the beginning of the task runs (Fig. 2D and Fig. S1). Uniquely, State 5 had significantly higher occupancy rates (67 ± 31 %) and mean lifetimes (12.8 ± 6.6 s) than any other states during the first trial of the task runs (all $ps<0.05$, two-tailed *t*-test, FDR-corrected, Fig. S3), suggesting its role in initiating task-set

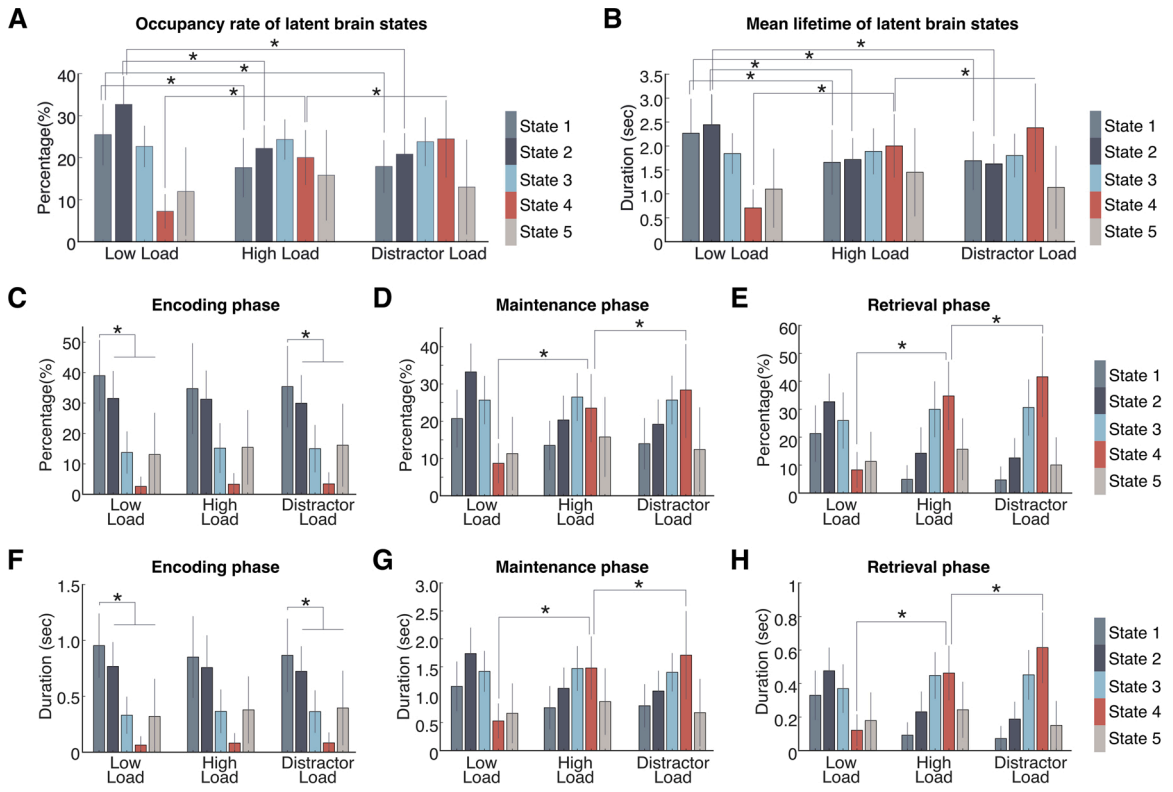

Fig. 4. Occupancy rates and mean lifetimes of latent brain states across task conditions and phases. **(A)** Occupancy rate and **(B)** mean lifetimes of latent brain states change significantly across low-load (LL), high-load (HL) and distractor-load (DL) conditions. Notably, the occupancy rate and mean lifetime of State 4 increased significantly as load demand increases. Occupancy rates of the latent brain states for **(C)** encoding, **(D)** maintenance, and **(E)** retrieval phases of the Sternberg task. Each phase is characterized by a mixture of brain states with distinct occupancies: The Encoding phase was dominated by States 1 and 2, such that State 1 showed a significantly higher occupancy rate than State 2 in LL and DL conditions. The maintenance phase of the LL condition was dominated by States 2 and 3, whereas the maintenance phase of HL and DL conditions were dominated by States 2, 3, and 4. During the maintenance and retrieval phases, the occupancy rate of State 4 increased significantly with cognitive load. Mean lifetime of the latent brain states for **(F)** encoding, **(G)** maintenance, and **(H)** retrieval phases of the Sternberg task. During the maintenance and retrieval phases, both occupancy rate and mean lifetime of State 4 increased significantly with cognitive load. Data represent as mean and standard deviation (mean ± SD). $^{*}p < 0.05$. two-tailed *t*-test, FDR-corrected.

reconfiguration for upcoming cognitive challenge. Taken together, these results demonstrate that latent brain states are characterized by unique cognitive-phase and load-dependent temporal properties.

3.7. Transition properties of latent brain states: state switch paths for different WM load conditions

To investigate transition paths of latent brain states during working memory, we used BSDS-derived state transition matrices for each participant. We first examined the stability of brain states by calculating the likelihood that a brain state remains the same brain state from a time point t to the next time point $t + 1$. This analysis revealed that all the five brain states persisted and were stable over time (Fig. 5A). We also found that latent brain states are constrained in the way they can switch between each other. For example, State 1, the brain state associated with stimulus encoding, cannot directly transit to State 4, the brain state associated with maintaining and retrieving information, but instead had to pass through States 2 and 3 or through State 5 (Fig. 5B). The most likely switching path in the LL condition consisted of transitioning from State 1 to 2 to 3 (Fig. 5C and D). In contrast, the most likely switching paths in both the HL and DL conditions consisted of transitioning from State 1 to 2 to 3 to 4 (Fig. 5C and D). Our findings demonstrate that state transitions depend on cognitive phase and task conditions.

3.8. Dynamic functional connectivity patterns distinguish latent brain states and switch paths

To analyze dynamic functional connectivity patterns associated with each latent brain state, we conducted classification analysis to determine whether multivariate patterns of functional connectivity can differentiate between latent brain states. We found that classifiers trained on functional connectivity accurately distinguish latent brain states (average accuracy = 91.1 %, all $ps = 0.002$, permutation test, Table S2). We then conducted univariate link-specific analyses to identify functional connectivity patterns that distinguished between latent brain states. We focused on the most likely switching path from encoding to retrieval in the HL and DL conditions (i.e., State 1 to 2 to 3 to 4, Fig. 5C and D) and examined changes in dynamic functional connectivity associated with these state transitions (all $ps<0.05$, two-tailed *t*-test, FDR-corrected) (Fig. 5E). We found that State 1, which dominates the encoding phase, has increased functional connectivity of the left caudate with the DLPFC and DMPFC, and left AI, compared to State 2, an intermittent switching state. State 3, which showed increased occurrence in the maintenance and retrieval phases of all three load conditions, had increased connectivity between DLPFC and left AI and thalamus compared to State 2. State 4, which exhibited load effect in maintenance and retrieval, had increased connectivity between the left caudate, and DLPFC and DMPFC, as well as between right caudate and right AI compared to State 3. These results suggest that connectivity changes in prefrontal-basal ganglia circuits play an important role in switching between latent brain states.

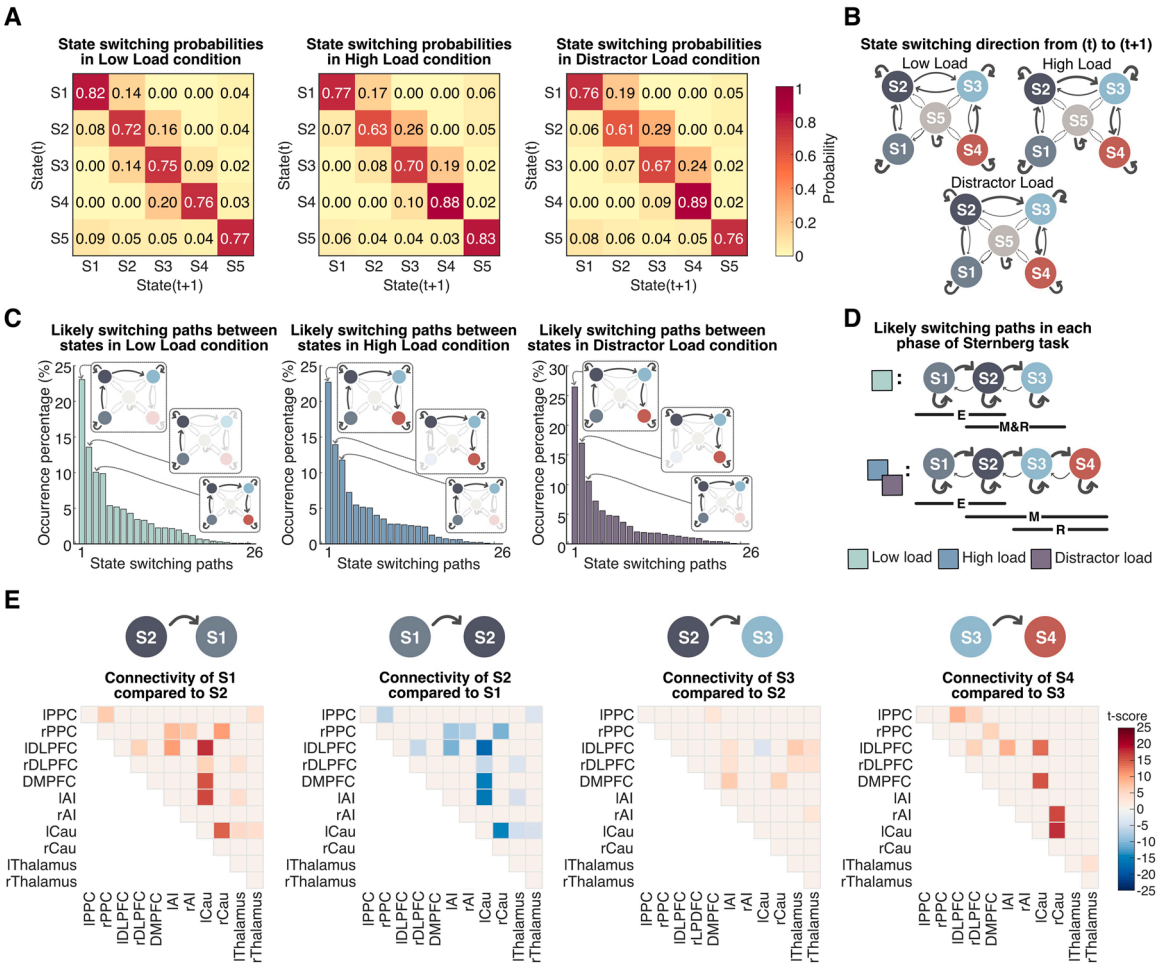

Fig. 5. Dynamic switching properties of latent brain states and functional connectivity patterns of each latent brain state. **(A)** State switching probabilities between the five latent brain states in low-load (LL), high-load (HL) and distractor-load (DL) conditions. The switching probability, also called transition matrix, is defined as the probability that a brain state at time point *t* remains within the same state or switches to one of the other four states at the next time point *t*+1. **(B)** State switching probability diagrams illustrating specific state switching characteristics between latent brain states in LL, HL, and DL conditions. State 1, a key state for stimulus encoding, does not switch directly to State 4, a key state for maintaining and retrieving information, in the HL and DL conditions. The most likely switch path from State 1 to 4 is through States 2 and 3. Line widths indicate switching probabilities between two latent brain states such that a heavier line width indicates a more likely switching probability. **(C)** Analysis of likely switching paths in each load condition. The most likely switching paths in the low-load condition were different from the most likely switching path of the high- and distractor-load conditions. **(D)** The most likely switch path in each phase of the Sternberg task for the three load conditions. Across the three phases, the most likely switching path in the low-load condition consisted of switching from State 1 to 2 to 3, whereas the most likely switching paths in the high and distractor conditions consisted of switching from State 1 to 2 to 3 to 4. **(E)** Specific circuits that distinguish functional connectivity patterns of latent brain states during the transition from State 1, which dominates the encoding phase, to State 4, which dominates the maintenance and retrieval phases, which has the most likely switching path from State 1 to 2 to 3 to 4. State transitions were characterized by dynamic changes in functional connectivity of the caudate nucleus with the prefrontal cortex (all *ps* < 0.05, two-tailed *t*-test, FDR-corrected).

3.9. Effect of age on brain state dynamics in older adults

Next, we investigated how age is associated with brain state dynamics, with focus on four temporal properties of latent brain states: state transition, state switch path, state mean lifetime, and state posterior probability.

First, we examined onset of state transition after the offset of the encoding phase, during which attention is shifted from external stimuli (encoding phase) to internal representation of stimuli (maintenance). We found that state transition onsets from State 1 (i.e., encoding-associated state) to State 2 (i.e., intermittent switching state) after the encoding phase is significantly shorter in HL (3.11 s) and DL (3.15 s) than LL conditions (LL: 3.65 s) (all *ps*<0.001, two-tailed *t*-test, Fig. 6A), reflecting higher maintenance demands in HL and DL conditions in comparison to the LL condition. Crucially, State 1 to 2 transition onset in the DL condition was positively correlated with age ($r = 0.38$, $p = 0.01$, *Pearson*'s correlation, Fig. 6A). Because participants not only needed to encode stimuli but also suppress distractors during the encoding phase in the DL condition, this result suggests that older age is associated with requiring more time to suppress distractors and complete encoding of task-relevant stimuli.

We then investigated how age affects state switching paths. Specifically, we examined the relation between age and the occurrence rate of state switch paths across participants, with a focus on the two state switching paths that dominated HL and DL conditions (i.e., State 1 to 2 to 3 to 4; State 2 to 3 to 4). We found that the total occurrence rate of these two state switch paths in the DL condition was negatively correlated with age (r=-0.37, $p = 0.02$, *Pearson*'s correlation, Fig. 6B), suggesting that older age is associated with reduced likelihood of following these two common state switch paths required to complete the working memory task. Notably, these two paths include the states that dominate the maintenance phase (States 3 and 4, Fig. 4D and G), suggesting that age impacts optimal paths associated with task maintenance.

We further examined whether age specifically affects mean lifetime

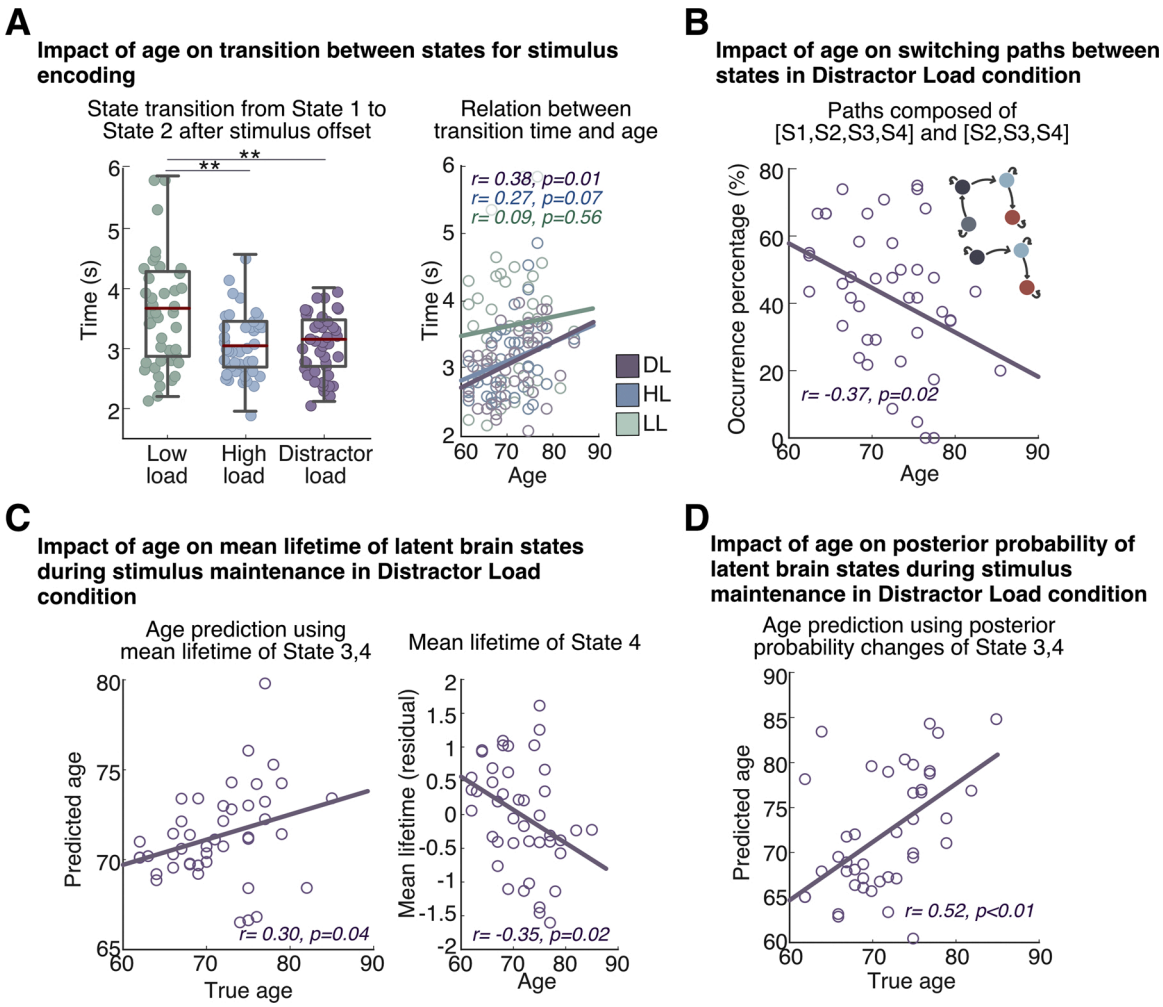

Fig. 6. Inflexible brain state dynamics associated with age. **(A)** Age impacts transitions between latent brain states associated with stimulus encoding in healthy older adults. Participants showed stimulus-encoding related state transitions from State 1 to 2 in low-load (LL), high-load (HL), and distractor-load (DL) conditions. State transition times were significantly shorter in HL and DL than LL conditions, respectively, reflecting the higher maintenance demands in HL and DL compared to LL conditions (left). Encoding-related state transition time increased with age in the DL condition (right). Data represent mean and standard deviation (mean ± SD). **(B)** Age impacts state switching paths taken by the participants during the DL condition. We examined the relation between age and the occurrence rate of state switch paths that dominated HL and DL conditions: State 1 to 2 to 3 to 4 and State 2 to 3 to 4. We found that the total occurrence rate of these two state switch paths decreased with age. **(C)** Prediction based on mean lifetime of States 3 and 4 during the maintenance phase in the DL condition (left). Mean lifetime of State 4, which is differentially engaged during the maintenance and retrieval phases of the DL condition, was negatively correlated with age (right). **(D)** Prediction based on posterior probability of States 3 and 4 during the maintenance phase in the DL condition. $^{**}p < 0.001$.

of States 3 and 4 during the maintenance phase in the DL task condition. We trained a multiple linear regression model with LOOCV to evaluate the model by computing the similarity between predicted age and true age. This analysis revealed a significant correlation between predicted age and true age ($r = 0.30$, $p = 0.04$, *Pearson*'s correlation, Fig. 6C). Correlation analysis revealed that age was negatively correlated with mean lifetime of State 4 (r=-0.35, $p = 0.02$, *Pearson*'s correlation, Fig. 6C). To further demonstrate the robustness of our findings, we replicated the same analysis using the posterior probabilities of States 3 and 4. Again, we found a significant correlation between predicted age and true age ($r = 0.52$, $p < 0.001$, *Pearson*'s correlation, Fig. 6D).

Taken together, these results demonstrate that within healthy older adults, age is negatively related to brain state dynamics associated with the maintenance phase.

3.10. Latent brain state dynamics predicts cognitive flexibility

Next, we used canonical correlation analysis (CCA) to probe the relationship between brain state dynamics and cognitive flexibility. CCA estimates the linear relationship between two sets of variables by finding an optimal linear combination for each of the sets so that these linear combinations (referred to as canonical variates) are maximally correlated (Hotelling, 1992; Smith et al., 2015). For CCA, brain dynamic measures included mean lifetimes of all latent brain states except State 5 because of its low occurrence rate throughout all cognitive phases and task conditions; cognitive measures consisted of TMT_A Time, which measures processing speed, TMT_{B-A} Time, which measures attention switching, and Stroop Color-Word time, which measures inhibitory control. Sex and education level were regressed out from all brain and cognitive measures included in the analysis.

CCA determined pairs of canonical variates such that brain dynamic measures and cognitive measures co-vary in a similar way across participants. We refer to each pair of variates as a mode of co-variation (Smith et al., 2015). Statistical significance of canonical correlations of each CCA mode was computed through permutation testing. This analysis revealed a single highly significant CCA mode between the 1st brain canonical variate and 1st cognitive canonical variate (*canonical correlation* = 0.83, $p_{FWE} = 0.002$ using permutation testing, Fig. 7A) and the LOOCV further demonstrated that our CCA model can predict cognitive flexibility on unseen data ($r = 0.63$, $p = 0.03$, *Pearson*'s

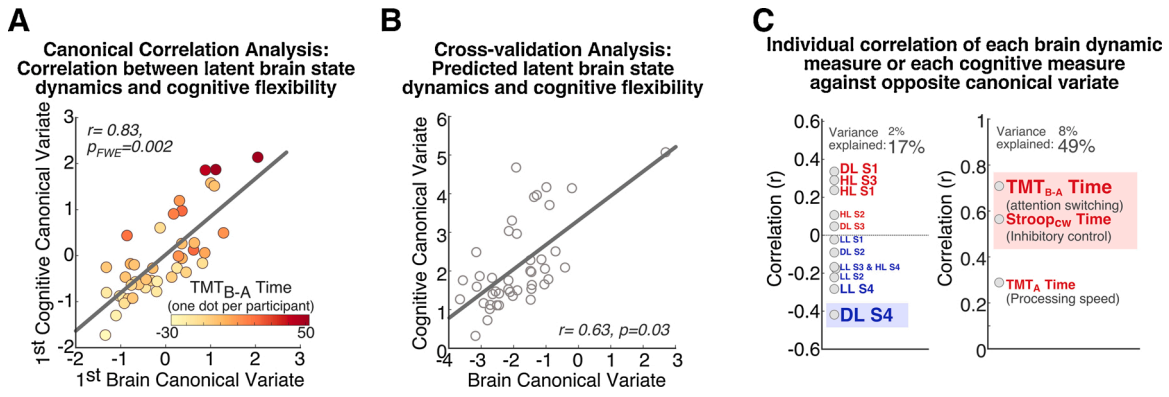

Fig. 7. Relation between brain and cognitive inflexibility. **(A)** Canonical correlation analysis (CCA) revealed a significant mode of covariation between dynamic brain measures of latent brain state dynamics, assessed using mean lifetimes of latent brain states, and standardized measures of cognitive flexibility, assessed using TMT_A Time, TMT_{B-A} Time, and Stroop Color-Word Time. Each dot represents an individual participant and an example cognitive measure (TMT_{B-A} Time) showed its high correlation with the canonical variates. **(B)** Prediction analysis performed using leave-one-out cross-validation revealed that, based on mean lifetimes of the four latent brain states, our CCA model can predict cognitive flexibility on unseen data. **(C)** Correlations between brain dynamic measures (i.e., mean lifetimes of latent brain states in LL, HL, and DL conditions) and 1st cognitive canonical variate (left). Correlations between cognitive measures and 1st brain canonical variate (right). Colored boxes indicate statistical significance of correlation ($p < 0.05$, FDR-corrected). Font size indicates variance explained by the opposite canonical variate.

correlation, Fig. 7B).

To further evaluate the relation between brain state dynamics and cognitive flexibility, we examined the canonical weights of the cognitive measures constituting the 1st cognitive canonical variate. The canonical weights of the cognitive measures were all positive (Fig. S4). Since the cognitive measures represent the task completion time of TMT and Stroop tests, a lower value of the 1st cognitive canonical variate indicates greater cognitive flexibility. Additional analysis revealed that the mean lifetime of State 4 in the DL condition was most strongly and negatively associated with the 1st cognitive canonical variate (r=-0.42, $p < 0.05$, *Pearson*'s correlation, FDR-corrected), indicating that longer dwelling time of the State 4 in the DL condition is associated with better cognitive flexibility (Fig. 7C).

Lastly, to investigate the specificity of the relationship between brain dynamic measures and cognitive flexibility, we applied the same analytical procedure used above to test whether brain dynamic measures are associated with other aspects of cognition that are less related to cognitive flexibility (i.e., memory, visuospatial functioning, and language). This analysis revealed no significant CCA mode between the brain state dynamics and the cognitive measures unrelated to cognitive flexibility (*canonical correlation* = 0.76, $p_{FWE} = 0.08$ using permutation testing, Fig. S5). Taken together, these results demonstrate that the temporal properties of latent brain states underlying working memory, and State 4 dynamics in particular, are closely and specifically associated with cognitive flexibility.

3.11. Brain state dynamics mediates relation between age and cognitive inflexibility

Finally, we tested the hypothesis that the relation between age and cognitive flexibility is mediated by brain state dynamics. Based on our findings above that the mean lifetime of State 4 in the DL condition was significantly associated with both age (Fig. 6C) and the 1st cognitive canonical variate reflecting cognitive flexibility (Fig. 7C), we specifically assessed whether mean lifetime of State 4 during the DL condition mediates the relation between age and cognitive flexibility while controlling for sex and education level. Mediation analysis with permutation testing revealed a significant indirect effect (indirect estimate = 0.03, $p = 0.02$, 95 % CI = 0.003 to 0.06) such that older age was associated with reduced mean lifetime of State 4 (path *a* in Fig. 8), which was in turn associated with reduced cognitive flexibility (path *b* in Fig. 8). The direct relation between age and cognitive flexibility was non-significant ($p = 0.28$). These results demonstrate that brain state dynamics is an intervening variable (Hayes, 2017, 2009) that mediates the relation between age and cognitive flexibility in healthy older adults.

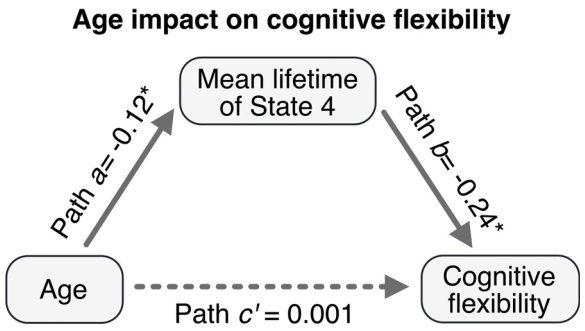

Fig. 8. Brain inflexibility mediates the relation between age and cognitive inflexibility in older adults. Mediation analysis revealed that the relation between age and cognitive inflexibility was mediated by flexible engagement of latent brain states. Brain flexibility was measured using mean lifetime of State 4 of the DL condition, the transient state engaged during the maintenance and retrieval phases of the Sternberg task. Cognitive flexibility was assessed using the 1st cognitive canonical variate (Fig. 7A). *$p < 0.05$.

3.12. Replication of findings using independent resting-state fMRI network derived ROIs

To examine the robustness of our findings with respect to ROI selection, we conducted additional analyses using independent cognitive control-related brain regions. We repeated all the above analyses using functional clusters from an independent study in which brain networks were derived using ICA on resting-state fMRI (Shirer et al., 2012). All major findings were replicated with this more general resting-state network-derived choice of ROIs (see Supplementary Results for details).

3.13. Control analyses using task-irrelevant brain regions

To further investigate the specificity of our findings with respect to prefrontal and parietal brain areas involved in cognitive control and working memory, we then repeated all the analyses using brain regions that are not expected to covary with task demands, including auditory, somatosensory, and visual networks (Fig. S7A). We found that none of the findings reported above were observed with these task-irrelevant ROIs (see Supplementary Results for details). Taken together, these

results demonstrate the specificity of frontal and parietal cognitive control ROIs for our findings.

4. Discussion

We used a novel Bayesian switching dynamical system (BSDS) model, and ultrafast temporal resolution (TR = 490 ms) whole-brain fMRI data from cognitively normal older adults (ages 60–85), to identify latent brain states and characterize dynamic state changes as a function of cognitive load and distinct phases of a Sternberg working memory task (Fig. 1). BSDS identified distinct load and phase-dependent dynamic latent brain states, each exhibiting unique temporal profiles and dynamic connectivity patterns. Our findings reveal, for the first time, a dynamic profile of the evolution of latent brain states and functional circuits associated with the encoding, maintenance and retrieval phases of the Sternberg task. We derived measures of brain flexibility using dynamic properties of latent brain states during working memory and found a significant negative effect of age on engagement of task-relevant dynamic latent brain states during working memory. Our analyses revealed increased brain inflexibility and greater inability to update information in working memory with age in healthy older adults. We further demonstrate that weak engagement of brain states impairs performance, and provide novel evidence for a relation between brain inflexibility and cognitive deficits in older adults. Finally, these findings were replicated using functional clusters from an independent study in which brain regions were obtained from salience network, fronto-parietal network, default mode network, and dorsal attention network with independent component analysis on resting-state fMRI (Shirer et al., 2012). Critically, our findings identify a latent brain mechanism by which age impairs cognitive flexibility in older adults and demonstrate that brain inflexibility mediates the relation between age and cognitive flexibility.

4.1. Dynamic temporal evolution of latent brain states associated with working memory phase

The first goal of our study was to identify latent brain states and characterize dynamic state changes as a function of cognitive load and the three distinct encoding, maintenance, and retrieval phases of the Sternberg working memory task. Human electrophysiological studies have revealed distinct activation and connectivity patterns associated with encoding, maintenance, and retrieval processes (Jensen and Lisman, 1998; Bashivan et al., 2014; Zakrzewska and Brzezicka, 2014), but the anatomical correlates have been hard to discern using scalp EEG recordings. In contrast, fMRI studies have typically not had the temporal resolution to disentangle brain responses associated with distinct phases (Ghuman and Martin, 2019; Glover, 2011), and, moreover, most previous studies have simply assumed that brain states are aligned with externally-driven task conditions and trial phases. We tested this assumption by examining how latent brain states emerge during working memory performance.

We leveraged one of the highest temporal resolutions to date of whole-brain functional neuroimaging, with a sub-second sampling rate, and a novel unsupervised learning algorithm to identify latent brain states and their temporal evolution associated with the Sternberg task. Intriguingly, we found distinct temporal profiles of latent brain states associated with the three cognitive phases in the Sternberg task. First, the encoding phase was dominated by States 1 and 2 (Fig. 4C and F). State 1 showed a transient response such that its rise and fall was aligned with the encoding phase but its occupancy rate during the encoding phase was not dependent on cognitive load, suggesting a role in initiation of encoding and disengagement when cognitive resources shift from processing external input to maintaining internal representation of stimuli. State 2 also had high occupancy rate during the encoding phase. In contrast to State 1, however, the rise and fall of occupancy rate of State 2 was not aligned with the encoding phase. The occupancy rate of State 2 remained high throughout the delay period and the encoding phase, dropping only after the encoding phase in high- and distractor-load working memory conditions but not in the low-load condition. This pattern of temporal evolution across task phase and cognitive load suggests that State 2 is differentially engaged when the cognitive load is low. State 2 also serves as an intermediate switching state that facilitates transitions between State 1 which dominates the encoding phase and State 3 that dominates the maintenance phase (see Supplementary Information for details on constraints on state switch paths).

Second, the maintenance and retrieval phases were dominated by States 3 and 4, which showed higher occupancy rates than the other latent brain states (Fig. 4D, E, G and H). The occupancy rates of both states were also higher in the maintenance and retrieval phases than the encoding phase. However, States 3 and 4 differed in their load-dependencies. Specifically, State 4 was load-dependent such that its occupancy rate was higher during DL than HL and HL than LL conditions. Furthermore, its occupancy rate dropped dramatically during inter-trial-interval (ITI) after the response phase (Fig. S2). In contrast, occupancy rates of State 3 were similar between three cognitive load conditions and remained stable across maintenance and retrieval phases. These findings suggest that State 4 may play a more crucial role in actively refreshing memorized items and searching for items to match the probe whereas State 3 may represent a passive maintenance process.

Third, while State 5 had overall low occupancy rate, it showed significantly higher occupancy than the other states in the first trial of each task run (Fig. S3). This suggests that State 5 may play a role in engaging latent brain states into an active task mode.

Lastly, we found that the temporal profiles of latent brain states in each load condition could predict cognitive phases with high accuracy, providing additional validation of distinct task-state profiles. Taken together, our findings reveal, a dynamic profile of the evolution of latent brain states associated with distinct phases of the Sternberg task. Further analyses of these temporal profiles were used to determine quantitative measures of brain flexibility in each participant, as described below.

4.2. Distinct functional circuits associated with latent brain states

The second goal of our study was to identify functional circuits associated with latent brain states in relation to cognitive load and the three distinct encoding, maintenance, and retrieval phases of the Sternberg working memory task. Each latent brain state is characterized by a distinct pattern of functional connectivity in the cognitive control network examined here. Classification analyses confirmed that multivariate patterns of inter-regional functional connectivity could accurately distinguish between the five latent brain states (Table S2). The basal ganglia circuit models suggest that cortico-striatal interactions act as a gate to select and update information in working memory (Chatham et al., 2014). Previous studies have demonstrated that the basal ganglia circuit is not only important for selectively encoding sensory information, but also plays a role in selective output gating (McNab and Klingberg, 2008). Our study extends these previous findings and provides insight into dynamical connectivity in cortico-striatal circuits during working memory.

Crucially, in both the HL and DL conditions, BSDS identified the most likely state switching path from encoding to maintenance and retrieval phases as State 1 to 2 to 3 to 4 (Fig. 5C). By examining dynamic connectivity changes during state transitions in this common state switching path, we found dynamic connectivity differences in prefrontal-striatum circuits between States 1 and 2 (i.e., encoding to an intermittent switching state), States 2 and 3 (i.e., an intermittent switching state to passive maintenance and retrieval), and States 3 and 4 (i.e., a passive maintenance and retrieval state to load dependent maintenance and retrieval), including dynamic interaction between caudate and DLPFC and DMPFC (Fig. 5E). States 3 and 4, in particular, were dominant in maintenance and retrieval phases but had functional dissociations demonstrated by load-dependent (State 4) vs. –independent (State 3)

characteristics. This pattern suggested that State 4 plays a role in refreshing and updating internal representation of stimuli whereas State 3 plays a role in passive maintenance. Indeed, by contrasting dynamic connectivity patterns between States 3 and 4, we found that State 4 has increased dynamic interactions between left caudate and left DLPFC and between left caudate and DMPFC in comparison to State 3. This suggests that State 4 involves more prefrontal-striatal interaction, which may underlie memory updating and refreshing. State 4 also has greater prefrontal-parietal interactions than State 3, which is consistent with the engagement of fronto-parietal network during working memory. Together, our findings identify a dynamic context dependent state and prefrontal-subcortical-parietal network that plays an essential role during working memory through refreshing and updating internal representations of external stimuli.

4.3. Brain inflexibility increases with age in healthy older adults

The third goal of our study was to investigate how brain flexibility, assessed through dynamic latent brain state properties underlying working memory, are affected by normal aging in older adults between ages 60–85 years. Our analysis revealed a significant negative impact of age on transitions between latent brain states characterized by slower transitions from State 1 to 2 in the DL condition, which requires encoding of task-relevant stimuli while suppressing distractors (Fig. 6A). These results are consistent with, and extend, previous findings of slower encoding of information (Zanto et al., 2010; Salthouse, 1996, 2016) and increased difficulty with top-down suppression of distractors (Clapp and Gazzaley, 2012) with age in older adults. We also found reduced likelihood of transitioning through the two dominant state switching paths in the DL condition, e.g. State 1 to 2 to 3 to 4 and State 2 to 3 to 4 with age (Fig. 6B). Taken together, these results demonstrate more fragmented transitions between latent brain states and provide novel quantitative evidence for increased brain inflexibility with age in healthy older adults.

We also examined whether mean lifetimes of latent brain states during working memory changed with age. A trained multiple linear regression model can accurately predict the age of a left-out participant (Fig. 6C). Further analysis revealed that the mean lifetime of State 4 was negatively correlated with age, suggesting that older participants have more difficulty in engaging a key load-dependent latent brain state during maintenance and retrieval (Fig. 6C). Our findings converge with and extend findings suggesting that the ability to update information in working memory may be specifically reduced with age (Lubitz et al., 2017; Zuber et al., 2019). These results reveal a significant effect of age on brain flexibility and context-specific engagement of task-relevant dynamic latent brain states during working memory.

4.4. Brain inflexibility, latent brain state dynamics and cognitive inflexibility

The fourth goal of our study was to determine how brain inflexibility impacts cognitive inflexibility. To address this, we examined the relation between engagement of dynamic brain states and performance on multiple neuropsychological tests that are commonly used to examine cognitive flexibility (Bowie and Harvey, 2006; Rabin et al., 2005). Canonical correlation analysis (CCA) revealed a significant linear relationship between dwell times of dynamic brain states and a composite measure of cognitive flexibility (Fig. 7A). Cross-validation analysis further demonstrated the robustness of the CCA model such that the trained model could accurately predict brain-behavior relationships in unseen data (Fig. 7B). We also found that longer dwelling time of State 4 in the DL condition was associated with better cognitive flexibility (Fig. 7C). These results suggest that weak engagement of task-phase-specific transient brain states impairs performance, and provide novel evidence for a link between brain and cognitive inflexibility in older adults.

4.5. Brain inflexibility mediates the relation between age and cognitive flexibility in older adults

The final goal of our study was to determine whether brain inflexibility mediates the relation between age and cognitive flexibility in healthy older adults. We evaluated the direct effects of age on cognitive inflexibility and contrasted this with a model in which brain inflexibility mediated the relation between age and cognitive inflexibility. We did not find a direct effect of age on cognitive flexibility. Rather, mediation analysis revealed a significant indirect path between age and cognitive flexibility via reduced mean lifetime of State 4 in the DL condition (Fig. 8). This result indicates that older age is associated with cognitive inflexibility through reduced engagement of State 4, the transient brain state involved in refreshing and updating internal representation of stimuli, particularly in high cognitive load contexts. It should be noted that despite some arguments to the contrary (Gelfand et al., 2009), a significant total (or direct) effect is not a prerequisite for a significant and interpretable mediation effect (Hayes, 2017, 2009; Rucker et al., 2011; MacKinnon et al., 2000, 2002) Furthermore, simulations have shown that bootstrapping is a powerful method for testing the effects of intervening variables and characterizing sources of variability (Hayes, 2017; Williams and MacKinnon, 2008). Critically, our results reveal a latent mechanism by which brain inflexibility mediates the relation between age and cognitive flexibility.

5. Conclusion

We used Bayesian switching dynamical system (BSDS) model to uncover latent time-varying and context-dependent brain states and quantify brain inflexibility in a quantitatively rigorous manner. Our study provides a novel neurocomputational framework for investigating dynamic circuit processes underlying brain inflexibility and age-related cognitive changes. The approach and methods developed here may be useful for probing brain inflexibility in neurological and psychiatric disorders across the lifespan.

Author contributions

Conceptualization: B.L., W.C., C.B.Y., K.L.P., V.M.; Methodology: B. L., W.C., R.Y., V.M.; Data acquisition: S.R., J.K., V.S., V.W.H., K.L.P.; Investigation: B.L., W.C., R.Y., V.M.; Writing: B.L., W.C., C.B.Y., R.Y., V. W.H., K.L.P., V.M.

Declaration of Competing Interest

The authors declare no competing interests.

Acknowledgments

This research was supported by grants from the Stanford ADRC, National Institute of Health (P50 AG047366, P30 AG066515, EB02290, NS086085, MH121069), and generous support of the Scully Foundation and the John Blume Foundation.

Appendix A. The Peer Review Overview and Supplementary data

The Peer Review Overview associated with this article can be found in the online version, at doi:https://doi.org/10.1016/j.pneurobio.2021.102180.

References

Altamura, M., et al., 2007. Dissociating the effects of Sternberg working memory demands in prefrontal cortex. Psychiatry Res. Neuroimaging 154, 103–114.

Bashivan, P., Bidelman, G.M., Yeasin, M., 2014. Spectrotemporal dynamics of the EEG during working memory encoding and maintenance predicts individual behavioral capacity. Eur. J. Neurosci. 40, 3774–3784.
Bassett, D.S., et al., 2011. Dynamic reconfiguration of human brain networks during learning. Proc. Natl. Acad. Sci. U. S. A. 108, 7641–7646.
Borella, E., Carretti, B., De Beni, R., 2008. Working memory and inhibition across the adult life-span. Acta Psychol. 128, 33–44.
Bowie, C.R., Harvey, P.D., 2006. Administration and interpretation of the trail making test. Nat. Protoc. 1, 2277–2281. https://doi.org/10.1038/nprot.2006.390.
Braun, U., et al., 2015. Dynamic reconfiguration of frontal brain networks during executive cognition in humans. Proc. Natl. Acad. Sci. U. S. A. 112, 11678–11683.
Braver, T.S., West, R., 2008. Working Memory, Executive Control, and Aging.
Cai, W., Ryali, S., Chen, T., Li, C.-S.R., Menon, V., 2014. Dissociable roles of right inferior frontal cortex and anterior insula in inhibitory control: evidence from intrinsic and task-related functional parcellation, connectivity, and response profile analyses across multiple datasets. J. Neurosci. 34, 14652–14667.
Cai, W., et al., 2019. Hyperdirect insula-basal-ganglia pathway and adult-like maturity of global brain responses predict inhibitory control in children. Nat. Commun. 10, 1–13.
Chang, C.-C., Lin, C.-J., 2001. LIBSVM: A Library for Support Vector Machines. Software available at http://www.csie.ntu.edu.tw/~cjlin/libsvm. (2001).
Chang, C., Crottaz-Herbette, S., Menon, V., 2007. Temporal dynamics of basal ganglia response and connectivity during verbal working memory. Neuroimage 34, 1253–1269.
Chatham, C.H., Frank, M.J., Badre, D., 2014. Corticostriatal output gating during selection from working memory. Neuron 81, 930–942.
Clapp, W.C., Gazzaley, A., 2012. Distinct mechanisms for the impact of distraction and interruption on working memory in aging. Neurobiol. Aging 33, 134–148.
Cohen, J.R., D'Esposito, M., 2016. The segregation and integration of distinct brain networks and their relationship to cognition. J. Neurosci. 36, 12083–12094.
Craft, S., et al., 1996. Memory improvement following induced hyperinsulinemia in Alzheimer's disease. Neurobiol. Aging 17, 123–130.
Cribben, I., Haraldsdottir, R., Atlas, L.Y., Wager, T.D., Lindquist, M.A., 2012. Dynamic connectivity regression: determining state-related changes in brain connectivity. Neuroimage 61, 907–920.
D'Esposito, M., Postle, B.R., 2015. The cognitive neuroscience of working memory. Annu. Rev. Psychol. 66.
Dajani, D.R., Uddin, L.Q., 2015. Demystifying cognitive flexibility: implications for clinical and developmental neuroscience. Trends Neurosci. 38, 571–578.
Escrichs, A., et al., 2021. Whole-brain dynamics in aging: disruptions in functional connectivity and the role of the rich club. Cereb. Cortex 31, 2466–2481.
Everett, B., 2013. An Introduction to Latent Variable Models. Springer Science & Business Media.
Ezaki, T., Sakaki, M., Watanabe, T., Masuda, N., 2018. A ge-related changes in the ease of dynamical transitions in human brain activity. Hum. Brain Mapp. 39, 2673–2688.
Fan, L., et al., 2016. The human brainnetome atlas: a new brain atlas based on connectional architecture. Cereb. Cortex 26, 3508–3526.
Finc, K., et al., 2020. Dynamic reconfiguration of functional brain networks during working memory training. Nat. Commun. 11, 1–15.
Fox, E.B., 2009. Bayesian Nonparametric Learning of Complex Dynamical Phenomena. Massachusetts Institute of Technology.
Gazzaley, A., Cooney, J.W., Rissman, J., D'esposito, M., 2005. Top-down suppression deficit underlies working memory impairment in normal aging. Nat. Neurosci. 8, 1298–1300.
Gelfand, L.A., Mensinger, J.L., Tenhave, T., 2009. Mediation analysis: a retrospective snapshot of practice and more recent directions. J. Gen. Psychol. 136, 153–178.
Ghahramani, Z., Hinton, G.E., 1996. The EM algorithm for mixtures of factor analyzers. Technical Report CRG-TR-96-1. University of Toronto.
Ghuman, A.S., Martin, A., 2019. Dynamic neural representations: an inferential challenge for fMRI. Trends Cogn. Sci. 23, 534–536.
Glover, G.H., 2011. Overview of functional magnetic resonance imaging. Neurosurg. Clin. 22, 133–139.
Goldman-Rakic, P.S., 1995. Cellular basis of working memory. Neuron 14, 477–485.
Hayes, A.F., 2009. Beyond Baron and Kenny: statistical mediation analysis in the new millennium. Commun. Monogr. 76, 408–420.
Hayes, A.F., 2017. Introduction to Mediation, Moderation, and Conditional Process Analysis: a Regression-based Approach. Guilford publications.
Hedden, T., Gabrieli, J.D., 2004. Insights into the ageing mind: a view from cognitive neuroscience. Nat. Rev. Neurosci. 5, 87–96.
Heinzel, S., et al., 2016. Neural correlates of training and transfer effects in working memory in older adults. Neuroimage 134, 236–249.
Hofer, S.M., Alwin, D.F., 2008. Handbook of Cognitive Aging: Interdisciplinary Perspectives.
Hotelling, H., 1992. In Breakthroughs in Statistics 162-190. Springer.
Ivanova, I., Salmon, D.P., Gollan, T.H., 2013. The multilingual naming test in Alzheimer's disease: clues to the origin of naming impairments. J. Int. Neuropsychol. Soc. 19, 272–283.
Jensen, O., Lisman, J.E., 1998. An oscillatory short-term memory buffer model can account for data on the Sternberg task. J. Neurosci. 18, 10688–10699.
Keller, J.B., et al., 2015. Resting-state anticorrelations between medial and lateral prefrontal cortex: association with working memory, aging, and individual differences. Cortex 64, 271–280.
Kim, C., Cilles, S.E., Johnson, N.F., Gold, B.T., 2012. Domain general and domain preferential brain regions associated with different types of task switching: a meta-analysis. Hum. Brain Mapp. 33, 130–142.
Kitzbichler, M.G., Henson, R.N., Smith, M.L., Nathan, P.J., Bullmore, E.T., 2011. Cognitive effort drives workspace configuration of human brain functional networks. J. Neurosci. 31, 8259–8270.
Lainscsek, C., et al., 2019. Nonlinear dynamics underlying sensory processing dysfunction in schizophrenia. Proc. Natl. Acad. Sci. U. S. A. 116, 3847–3852.
Leonardi, N., Van De Ville, D., 2015. On spurious and real fluctuations of dynamic functional connectivity during rest. NeuroImage 104, 430–436.
Lubitz, A.F., Niedeggen, M., Feser, M., 2017. Aging and working memory performance: electrophysiological correlates of high and low performing elderly. Neuropsychologia 106, 42–51. https://doi.org/10.1016/j.neuropsychologia.2017.09.002.
MacKinnon, D.P., Krull, J.L., Lockwood, C.M., 2000. Equivalence of the mediation, confounding and suppression effect. Prev. Sci. 1, 173–181.
MacKinnon, D.P., Lockwood, C.M., Hoffman, J.M., West, S.G., Sheets, V., 2002. A comparison of methods to test mediation and other intervening variable effects. Psychol. Methods 7, 83.
McNab, F., Klingberg, T., 2008. Prefrontal cortex and basal ganglia control access to working memory. Nat. Neurosci. 11, 103–107.
Menon, V., D'Esposito, M., 2021. Prefrontal Cortex Networks in Cognitive Control. American College of Neuropsychopharmacology.
Murphy, A.C., Bertolero, M.A., Papadopoulos, L., Lydon-Staley, D.M., Bassett, D.S., 2020. Multimodal network dynamics underpinning working memory. Nat. Commun. 11, 1–13.
Myers, N.E., Stokes, M.G., Nobre, A.C., 2017. Prioritizing information during working memory: beyond sustained internal attention. Trends Cogn. Sci. 21, 449–461.
Owen, A.M., McMillan, K.M., Laird, A.R., Bullmore, E., 2005. N-back working memory paradigm: a meta-analysis of normative functional neuroimaging studies. Hum. Brain Mapp. 25, 46–59.
Park, D.C., et al., 2002. Models of visuospatial and verbal memory across the adult life span. Psychol. Aging 17, 299.
Possin, K.L., Laluz, V.R., Alcantar, O.Z., Miller, B.L., Kramer, J.H., 2011. Distinct neuroanatomical substrates and cognitive mechanisms of figure copy performance in Alzheimer's disease and behavioral variant frontotemporal dementia. Neuropsychologia 49, 43–48.
Poston, K.L., et al., 2016. Compensatory neural mechanisms in cognitively unimpaired P arkinson disease. Ann. Neurol. 79, 448–463.
Qian, J., Hastie, T., Friedman, J., Tibshirani, R., Simon, N., 2013. Glmnet for Matlab.
Rabin, L.A., Barr, W.B., Burton, L.A., 2005. Assessment practices of clinical neuropsychologists in the United States and Canada: a survey of INS, NAN, and APA Division 40 members. Arch. Clin. Neuropsychol. 20, 33–65.
Reuter-Lorenz, P.A., Sylvester, C.-Y.C., 2005. The cognitive neuroscience of working memory and aging. Cognitive Neuroscience of Aging: Linking Cognitive and Cerebral Aging, pp. 186–217.
Rocca, W.A., et al., 2011. Trends in the incidence and prevalence of Alzheimer's disease, dementia, and cognitive impairment in the United States. Alzheimer's Dementia 7, 80–93.
Rottschy, C., et al., 2012. Modelling neural correlates of working memory: a coordinate-based meta-analysis. Neuroimage 60, 830–846.
Rucker, D.D., Preacher, K.J., Tormala, Z.L., Petty, R.E., 2011. Mediation analysis in social psychology: current practices and new recommendations. Soc. Personal. Psychol. Compass 5, 359–371.
Salthouse, T.A., 1996. The processing-speed theory of adult age differences in cognition. Psychol. Rev. 103, 403.
Salthouse, T.A., 2009. When does age-related cognitive decline begin? Neurobiol. Aging 30, 507–514.
Salthouse, T.A., 2010. Selective review of cognitive aging. J. Int. Neuropsychol. Soc.: JINS 16, 754.
Salthouse, T., 2012. Consequences of age-related cognitive declines. Annu. Rev. Psychol. 63, 201–226.
Salthouse, T.A., 2016. Theoretical Perspectives on Cognitive Aging. Psychology Press.
Samu, D., Campbell, K.L., Tsvetanov, K.A., Shafto, M.A., Tyler, L.K., 2017. Preserved cognitive functions with age are determined by domain-dependent shifts in network responsivity. Nat. Commun. 8, 1–14.
Sánchez-Cubillo, I., et al., 2009. Construct validity of the Trail making Test: role of task-switching, working memory, inhibition/interference control, and visuomotor abilities. J. Int. Neuropsychol. Soc. 15, 438–450.
Scott, W.A., 1962. Cognitive complexity and cognitive flexibility. Sociometry 405–414.
Shakil, S., Lee, C.-H., Keilholz, S.D., 2016. Evaluation of sliding window correlation performance for characterizing dynamic functional connectivity and brain states. NeuroImage 133, 111–128.
Shine, J.M., et al., 2016. The dynamics of functional brain networks: integrated network states during cognitive task performance. Neuron 92, 544–554.
Shirer, W.R., Ryali, S., Rykhlevskaia, E., Menon, V., Greicius, M.D., 2012. Decoding subject-driven cognitive states with whole-brain connectivity patterns. Cereb. Cortex 22, 158–165.
Smith, S.M., et al., 2015. A positive-negative mode of population covariation links brain connectivity, demographics and behavior. Nat. Neurosci. 18, 1565.
Spadone, S., et al., 2015. Dynamic reorganization of human resting-state networks during visuospatial attention. Proc. Natl. Acad. Sci. U. S. A. 112, 8112–8117.
Stroop, J.R., 1935. Studies of interference in serial verbal reactions. J. Exp. Psychol. 18, 643.
Taghia, J., et al., 2018. Uncovering hidden brain state dynamics that regulate performance and decision-making during cognition. Nat. Commun. 9, 1–19.
Vidaurre, D., Smith, S.M., Woolrich, M.W., 2017. Brain network dynamics are hierarchically organized in time. Proc. Natl. Acad. Sci. U. S. A. 114, 12827–12832.

Williams, J., MacKinnon, D.P., 2008. Resampling and distribution of the product methods for testing indirect effects in complex models. Struct. Equ. Model. A Multidiscip. J. 15, 23–51.

Zakrzewska, M.Z., Brzezicka, A., 2014. Working memory capacity as a moderator of load-related frontal midline theta variability in Sternberg task. Front. Hum. Neurosci. 8, 399.

Zanto, T.P., Toy, B., Gazzaley, A., 2010. Delays in neural processing during working memory encoding in normal aging. Neuropsychologia 48, 13–25.

Zuber, S., et al., 2019. Explaining age differences in working memory: the role of updating, inhibition, and shifting. Psychol. Neurosci. 12, 191–208. https://doi.org/10.1037/pne0000151.